Cisplatin-induced Ototoxicity Is Mediated by Nitroxidative Modification of Cochlear Proteins Characterized by Nitration of Lmo4*□S

Samson Jamesdaniel[‡1], **Donald Coling**[‡], **Sneha Hinduja**[‡], **Dalian Ding**[‡], **Jun Li**[§], **Linda Cassidy**[‡2], **Gail M. Seigel**[‡2], **Jun Qu**[§], and **Richard Salvi**[‡]

From the ‡*Department of Communicative Disorders and Sciences, The State University of New York, Buffalo, New York 14214 and the* §*Department of Pharmaceutical Sciences, School of Pharmacy and Pharmaceutical Sciences, The State University of New York, Buffalo, New York 14260*

Background: Oxidative stress plays a causal role in cisplatin ototoxicity.
Results: Cisplatin induces nitration of cochlear proteins that correlate with measures of ototoxicity, and pharmacological inhibition of cochlear protein nitration attenuates ototoxic effects of cisplatin.
Conclusion: Nitroxidative modification of cochlear proteins is an important mediator of cisplatin ototoxicity.
Significance: Cisplatin-induced nitration of Lmo4 points to novel target genes related to stress responses.

Tyrosine nitration is an important sequel of cellular signaling induced by reactive oxygen species. Cisplatin is an anti-neoplastic agent that damages the inner ear through reactive oxygen species and by the formation of DNA adducts. This study reveals a correlation between cisplatin-mediated hearing loss and nitroxidative modification of cochlear proteins and is the first to report nitration of Lmo4. Cisplatin induced a dose-dependent increase in hearing loss in Wistar rats. A 10-15-dB decrease in distortion product amplitude and massive loss of outer hair cells at the basal turn of the cochlea was observed 3 days post-treatment after a 16 mg/kg dose. Cisplatin induced nitration of cellular proteins within the organ of Corti, spiral ganglion, and stria vascularis, which are known targets of cisplatin ototoxicity. Nitration of a 76-kDa cochlear protein correlated with cisplatin dose. The nitrated protein was identified as Lmo4 (LIM domain only 4) by MALDI-TOF (matrix-assisted laser desorption/ionization time of flight) mass spectrometry and confirmed by reciprocal immunoprecipitation and immunoblotting. Co-localization of nitrotyrosine and Lmo4 was particularly high in outer hair cell nuclei after cisplatin treatment. Cochlear levels of Lmo4 were decreased in rats treated with cisplatin. *In vitro* studies supported the repression of Lmo4 in nitroxidative conditions and the induction of apoptosis upon repression of Lmo4. Inhibition of cochlear protein nitration prevented cisplatin-induced hearing loss. As Lmo4 is a transcriptional regulator that controls the choice between cell survival and cell death, these results support the hypothesis that nitration of Lmo4 influences cisplatin-induced ototoxicity.

Reactive oxygen species, such as superoxide anions (1), are among the important factors that lead to cisplatin-mediated cell death. The cytotoxic effects of cisplatin occur primarily through apoptosis (2). In the cochlea, cisplatin activates the enzyme NOX3, which increases the production of superoxide radicals (3). Superoxide leads to the formation of hydrogen peroxide, which when catalyzed by iron forms the highly reactive hydroxyl radical and leads to damaging lipid peroxidation. Peroxynitrite, formed by the reaction of superoxide with nitric oxide, reacts with susceptible proteins to form nitrotyrosine, an indicator of oxidative damage to proteins (4). Protein nitration can also be derived by peroxidase-mediated mechanism (5). We previously reported that cisplatin increased the nitration of proteins in the cochlea (6). Immunodetection of nitrotyrosine has also been reported in auditory neurons of cisplatin-treated mice (7).

Ototoxicity due to cisplatin treatment is generally manifested as sensorineural hearing loss, which is usually bilateral, permanent, and dependent on the cumulative dose of cisplatin (8). Cisplatin-induced elevation of hearing threshold has been detected through the auditory brainstem response, whereas distortion product otoacoustic emissions (DPOAEs),[3] a measure of OHC function, are diminished in cisplatin treated rats (6). Platinated-DNA immunoreactivity is localized to the nuclei of OHC, the stria vascularis, spiral ligament (9–11), spiral ganglion neurons (12) predominantly in the basal turn of the organ of Corti (13). Pro-apoptotic signaling (14) and nitration of cochlear proteins (6) have been demonstrated in the cochlea within 48 h of cisplatin treatment. Nitration of tyrosine residues can produce catastrophic effects on protein function by blocking the ability of protein-tyrosine kinases to activate certain transcription factors (15). Despite the significant pathophysiological consequences attributed to protein nitration, the role of nitrated proteins in cisplatin-mediated toxicity is not well established.

[1] To whom correspondence should be addressed: Communicative Disorders and Sciences, 137 Cary Hall, 3435 Main St., The State University of New York, Buffalo, NY 14214. Tel.: 716-829-5297; Fax: 716-829-2980; E-mail: sj57@buffalo.edu.

[3] The abbreviations used are: DPOAE, distortion product otoacoustic emission; OHC, outer hair cells; IHC, inner hair cells; Lmo4, LIM domain only 4.

Tyrosine nitration is capable of causing vital changes in biological function as it modulates phosphorylation cascades and interactions with proteins and nucleic acids. Pathologic manifestations associated with protein nitration depend on the functional role of the specific proteins, whose nitration results in either loss or gain of function. Moreover, nitrated proteins are often targets for proteolytic degradation by the 20 S proteasome (16, 17). Hence, establishing the identity of nitrated proteins is of paramount importance to understand the functional implications of cisplatin-induced nitration of cochlear proteins. This study reports a correlation between cisplatin-induced hearing loss and nitration of inner ear proteins. We identify the major nitrated protein as Lmo4 and show that cisplatin induces Lmo4 nitration in a number of critical cell types including OHC, spiral ganglion neurons, and strial cells. The functional characteristics of Lmo4 coupled with its modulation and localization in the cochlea after cisplatin treatment points to an important role for nitrated Lmo4 in mediating cisplatin ototoxicity.

EXPERIMENTAL PROCEDURES

Animals—Three-month-old male Wistar rats, 0.3–0.35 kg, were obtained from Charles River Laboratories (Wilmington, MA). The animals were housed at the Laboratory Animal Facility of the University at Buffalo. The animals were maintained in a temperature-controlled room with a 12-h light/dark cycle and allowed free access to food and water. The experimental protocol was reviewed and approved by the University at Buffalo Institutional Animal Care and Use Committee. The animals were handled and treated according to guidelines established by the National Institutes of Health and the Institutional Animal Care and Use Committee at the University at Buffalo, the State University of New York.

Reagents—All reagents were purchased from Sigma unless noted otherwise.

Drug Administration—Cisplatin was administer following a standard protocol with some modifications (18). Briefly, rats were hydrated at least 1 h before treatment by subcutaneous injection of 15 ml of sterile saline (0.9%)/kg of body weight, then anesthetized with isoflurane (4% induction, 1.5% maintenance, both with 1 liter/min O_2) and injected with a single dose of cisplatin, 8, 12, or 16 mg/kg body weight, by intraperitoneal infusion of a 1 mg/ml solution in sterile saline at the rate of 10 ml/h. Control animals were infused with an equal volume of saline per kg of body weight. All of the animals were weighed and hydrated daily with a subcutaneous injection of saline, 15 ml/kg body weight, until they were sacrificed. Trolox, a water-soluble analog of vitamin E, was administrated following a standard protocol with some modifications (19). Trolox (100 mg/kg) was mixed with sterile saline (pH 7.2–7.4) and administered by intraperitoneal injection 1 h before and on the 1st and 2nd day after cisplatin treatment.

Distortion Product Otoacoustic Emissions—DPOAEs were measured after anesthetizing the animals with isoflurane (4% induction, 1.5% maintenance with 1 liter/min O_2). DPOAEs were elicited with two primary tones, f_1 and f_2 at an f_2/f_1 ratio of 1.2, holding $L_2 = L_1 - 10$ dB, for L_1 levels from 70 to 15 dB SPL in 5-dB increments. IHS-3738 high frequency transducers (Intelligent Hearing Systems, IHS, Miami, FL) were used to deliver f_1 and f_2. Frequency f2 varied from 4 to 32 kHz. Sound pressure levels was measured at the cubic difference frequency ($2f_1 - f_2$) using a ER10B+ probe microphone (Etymotic Research, Inc., Elk Grove Village, IL) and hardware-software from a Smart DPOAE System version 4.53 (IHS). The spectrum of each sweep was computed and averaged over 32 non-rejected sweeps. The noise floor was measured in a 24-Hz band surrounding $2f_1 - f_2$ (6).

Cochleograms—Animals were euthanized with CO_2 inspiration followed by decapitation. Afterward the cochlea was removed from its bulla and then slowly perfused with 4% paraformaldehyde in 0.1 M phosphate buffer (pH 7.2, 4 °C) through the round window and immersed in fixative for 3 h. Specimens were stained with Harris' hematoxylin solution. The cochlea containing the organ of Corti was dissected out as a flat surface preparation and mounted in glycerin on a glass slide. Missing inner hair cells (IHC) and OHC were counted over 0.24-mm intervals under a light microscope (400×). The cochleograms were generated showing the percent hair cell loss as a function of percent distance from the apex (20).

Protein Extraction—For cochlear protein extraction, the animals were anesthetized with CO_2 and decapitated, and the cochlear tissues (lateral wall, sensory epithelium, and bony modiolus) were dissected in ice-cold PBS. The tissue was homogenized in radioimmunoprecipitation assay buffer supplemented with 5 mM EDTA and phosphatase and protease inhibitors (all from Pierce). Homogenization was performed on ice in 1.5-ml homogenization tubes with fitted pestles (Kontes, Kimble Chase, Vineland, NJ) using a 50% duty cycle, 10-s pestle rotation twice with a 20-s interval. The homogenate was extracted on ice for 45 min and then centrifuged at $14,000 \times g$ for 10 min. For protein extraction from cultured cells, the cells were washed with PBS, suspended in radioimmunoprecipitation assay buffer, extracted on ice for 15 min, and centrifuged at $14,000 \times g$ for 15 min. Protein concentration of the supernatant was determined using the Bradford assay (21).

Subcellular Fractionation—Cytoplasmic and nuclear proteins were separated using the Subcellular Protein Fractionation kit (Pierce) following the manufacturer's protocol. Two pairs of cochleae were used to obtain each sample. Cytoplasmic proteins were minced and extracted in 500 μl of the cytoplasmic extraction buffer designed for selective cell membrane permeabilization and release of soluble cytoplasmic contents. Nuclear proteins were extracted in two steps. First, soluble nuclear proteins were extracted in 250 μl of nuclear extraction buffer, and then chromatin-bound nuclear proteins were extracted in 250 μl of the same buffer containing micrococcal nuclease and calcium chloride. Finally both nuclear fractions were pooled together. Then the cytoplasmic and nuclear fractions were concentrated using Vivaspin 500, 5-kDa molecular weight cutoff protein concentrators (GE Healthcare), and 10 μg of proteins were loaded in the gels.

Immunoblotting—Protein extracts were mixed with a lithium dodecyl sulfate sample buffer (Invitrogen) at a pH of 8.4, denatured by heating at 70 °C for 10 min, reduced with 500 mM dithiothreitol, and 20 μg of total protein was loaded in each lane of the gel. Proteins were separated on 4–12% gradient NuPage gels (Invitrogen) and transferred to polyvinylidene difluoride

(PVDF) membranes using the iBlot Dry Blotting System (Invitrogen). The PVDF membranes were then blocked with 0.1% I-Block (Applied Biosystems, Foster City, CA) and probed with either a monoclonal anti-nitrotyrosine or polyclonal anti-Lmo4 (Santa Cruz Biotechnology, Inc., Santa Cruz, CA) using chemiluminescence detection (Pierce). A Fuji model LAS 1000 imaging system (Stamford, CT) was used to visualize bands. Background-corrected bands (NIH Image J software) were normalized against actin bands obtained by stripping the membrane with 25 mM glycine (Bio-Rad) (pH 2.0), 1% lauryl sulfate (Fisher) and reprobing with an anti-actin monoclonal antibody (Millipore, Bellerica, MA). For negative controls, the membranes were incubated with sodium dithionite (100 mM in 100 mM sodium borate (pH 9.0) for 5 min) to reduce nitrotyrosine to aminotyrosine before immunoblotting (22). Differences in intensity were analyzed by one-tailed t tests. Correlations between dose and nitration levels were analyzed by linear regression, whereas the correlations between nitration and functional loss were assessed by Pearson correlation coefficient.

3'3'-Diaminobenzidine Tetrahydrochloride Staining of Cryosections—Cochlea was dissected out after anesthetizing the rats with a 1-ml intraperitoneal injection of Fatal-plus Solution (Vortech Pharmaceuticals, Dearborn, MI) followed by a transcardial perfusion with 0.1 M phosphate-buffered saline at pH 7.4 for 5 min and then with 10% phosphate-buffered formalin (4% formaldehyde, Fisher) for 15 min. The cochlea was fixed in formalin for 1 week and then decalcified with 10% EDTA for at least 3 days. After incubating the cochlea in 30% sucrose overnight, $40-50-\mu m$ cryosections were obtained at $-23\,°C$. The sections were blocked in PBS containing 10% normal horse serum, 1% bovine serum albumin, and 1% Triton-X for 30 min and incubated with the primary antibody for 2 h and biotinylated secondary antibody (Vector Laboratories, Burlingame, CA) for 1 h at room temperature. Then sections were treated with the avidin and biotin (Elite ABC-kit, Vector Laboratories) in PBS-Triton for 1 h and stained with 0.05% 3'3'-diaminobenzidine tetrahydrochloride with 0.3% nickel ammonium sulfate and 0.0015% H_2O_2 in Tris buffer (0.1 M Tris (pH 7.2)). The reaction was stopped with Tris buffer, and the sections were washed with PBS and mounted on slides.

Fluorescent Labeling of Surface Preparations—Co-localization of nitrotyrosine and Lmo4 in the cochlea was done by immunocytochemistry using confocal microscopy (23). Sensory epithelia were dissected from the cochleae, fixed in 10% buffered formalin for 1 h, and permeabilized in PBS + 1% v/v Triton X-100 for 30 min. The tissue was blocked in 5% v/v goat serum, 2% w/v bovine serum albumin in PBS for 1 h and incubated overnight at 4 °C in primary antibodies (mouse monoclonal anti-nitrotyrosine and rabbit polyclonal anti-LMO4). After three 5-min washes in PBS, tissue was incubated with secondary antibodies in blocking solution at room temperature for 1 h. Alexa Fluor 568 donkey anti-mouse IgG and Alexa Fluor 647 goat anti-rabbit IgG were obtained from Invitrogen/Molecular Probes (Carlsbad, CA). After secondary antibody incubation, tissue was washed and F-actin was labeled with fluorescein-conjugated phalloidin. Stained specimens were mounted on slides with ProLong Gold antifade reagent containing DAPI nuclear stain (Invitrogen/Molecular Probes) and examined using a Laser Scanning Microscope LSM 510 Meta (Carl Zeiss, Jena, Germany). Images were captured and analyzed with Zeiss LSM Image Examiner (Version 4.0.0.91).

Immunoprecipitation—A Dynabeads® Protein G kit (Invitrogen) was used to immunoprecipitate nitrated and Lmo4 proteins following the manufacturer's protocol. Extracts from whole cochlea (400 μg protein) were incubated with antibody (10 μg) bound to 50 μl of Protein G magnetic beads (30 mg/ml suspension) for 10 min at room temperature. The immune complexes bound to the beads were separated from other proteins using the magnetic properties of the beads. The bead-bound proteins were then eluted using elution buffer and denatured by boiling with gel loading buffer. The magnetic beads were removed before loading the precipitated protein sample onto the gel.

In-gel Tryptic Digestion—Immunoprecipitated nitrated proteins were digested using an In-Gel Tryptic Digestion kit (Pierce). The most prominent protein band from the 4–12% gradient NuPage one-dimension gel stained by Imperial protein stain (Pierce) was cut into to 2 × 2-mm pieces and destained with 25 mM ammonium bicarbonate containing 50% acetonitrile. Then the sample was reduced by incubation at room temperature for 10 min in 25 mM ammonium bicarbonate buffer containing 50 mM TCEP (tris(2-carboxyethyl)phosphine) and alkylated by incubation for 60 min in 100 mM iodoacetamide. The alkylated gel pieces were washed by adding 50 μl of acetonitrile and allowed to air-dry for 5–10 min. Finally the gel pieces were digested by incubation in 10 μl of trypsin in 25 mM ammonium bicarbonate buffer at a 10 ng/μl concentration at room temperature for 15 min. Peptides were extracted in 25 μl of 25 mM ammonium bicarbonate buffer by incubating at 30 °C overnight and concentrated using C-18 Zip tips (Millipore).

MALDI-TOF MS—The major nitrated cochlear protein was identified by MALDI-TOF mass spectrometry following a protocol employed to identify cochlear proteins in cisplatin toxicity (24). Concentrated tryptic peptides or peptide calibration standards (Bruker Daltonics, Billerica, MA) in 0.1% trifluoroacetic acid, 75% acetonitrile were spotted on a stainless steel target plate covered with a matrix made of saturated solution of α-cyano-4-hydroxy-cinnamic acid (Bruker) in 0.1% trifluoroacetic acid, 60% acetonitrile. Peptide masses were measured on a MALDI-TOF mass spectrometer (Biflex IV, Bruker). A Peptide Calibration Standard II (Bruker) was used for calibrating the instrument.

Peptide Mass Fingerprinting—The mass spectrum was viewed using m/z software (Genomic Solutions), and the masses of the monoisotopic peaks were analyzed to find appropriate matches. The Mascot online search engine was used to search the National Center for Biotechnology Information (NCBI) protein data base to compare the masses and facilitate the identification of nitrated proteins. The search parameters employed were: type of search, peptide mass fingerprint: enzyme, trypsin; modifications, none; mass values, monoisotopic; protein mass, unrestricted, peptide mass tolerance. ± 1.2 Da; contaminants excluded, trypsin; peptide charge state, MH+; max missed cleavages, 1; no. of entries, 8; accepted threshold score, >61 ($p < 0.05$).

MS/MS Analysis of Nitrated Lmo4—A suspension containing 0.2 mg/ml recombinant Lmo4 protein (OriGene, Rockville, MD) was nitrated by incubating with 0.17 mM peroxynitrite (Cayman Chemical, Ann Arbor, MI) in 25 mM Tris buffer (pH 7.3) for 30 min at 37 °C (25). Nitrated Lmo4 proteins were digested with trypsin, and tryptic peptides were separated and identified using a nano-LC coupled to a high resolution/accuracy Orbitrap/electron-transfer dissociation system. The details for sample preparation and dual-activation nano-LC/MS analysis are described in previous publications (26–28). Briefly, a precipitation of the sample was digested after an on-pellet-digestion protocol (26), where a dynamic flow nanospray interface was used to clean and digest the samples. A high resolution nano-LC separation was employed to resolve the tryptic peptides. The MS worked in a data-dependent mode in which one MS1 scan was followed by multiple dependent sequential MS2 scans. Collision-induced dissociation and electron-transfer dissociation methods were employed alternatively for peptide sequencing and localization of the nitration site(s) in Lmo4. The generated spectra was analyzed using BioWorks software (3.3.1, Thermo Scientific) with SEQUEST algorithm. The cutoff threshold was precursor mass error <15 ppm, Xcorr >1.7 for 1+, >2.2 for 2+, >3.2 for 3+, and >4 for 4+. Mass modification of +44.985 Da for tyrosine nitration was considered.

Cell Culture—MDA-MB231 (HTB-26, American Type Culture Collection, Manassas, VA), a human breast adenocarcinoma cell line that expresses LMO4, was grown in Liebovitz's L-15 medium (ATCC catalog no. 30-2008) with 10% fetal bovine serum (ATCC catalog no. 30-2020) at 37 °C in 100% room air. The cells were seeded into 6-well plates in Leibovitz's L15 + 10% FBS so that they would be 50–70% confluent at the time of transfection or peroxynitrite treatment.

Peroxynitrite Treatment—Cells were washed with Dulbecco's phosphate-buffered saline, supplemented with 0.8 mM MgCl$_2$, 1 mM CaCl$_2$, and 5 mM glucose, and incubated in 1 ml of 50 mM Na$_2$HPO$_4$, 90 mM NaCl, 5 mM KCl, 0.8 mM MgCl$_2$, 1 mM CaCl$_2$, and 5 mM glucose, pH 7.4, for 1–2 min. Then peroxynitrite was added to achieve the required concentration (0.25, 0.5, and 1 mM). Five minutes after peroxynitrite exposure, the buffer was removed, and the cells were washed with PBS. The cells were then incubated in L-15 medium supplemented with 10% FBS in atmospheric air at 37 °C and harvested 24 h after peroxynitrite treatment (29).

Cochlear Organotypic Culture—Cochleae from Sprague-Dawley rat pups were dissected in Hanks' balanced salt solution (1×, 14175, Invitrogen) at postnatal day 3. The lateral wall and auditory nerve bundles were removed, and the sensory epithelia containing the organ of Corti and spiral ganglion neurons were transferred onto a collagen-gel matrix as a flat surface preparation. The gel matrix was formed in a culture dish (Falcon 1008, BD Biosciences) with a drop (15 μl) of rat tail collagen (Type 1, BD Biosciences, 10× basal medium Eagle medium (Sigma B9638), 2% sodium carbonate, 9:1:1 ratio) at room temperature. Then 1.2 ml of a serum-free medium (consisting of 2 g of bovine serum albumin, 2 ml of serum-free supplement (Sigma I-1884), 4.8 ml of 20% glucose, 0.4 ml of penicillin G, 2 ml of 200 mM glutamine, and 190.8 ml of 1× basal medium eagle, Sigma B-1522) was added to the dish, and the cochlear explants were

placed in an incubator (Forma Scientific, #3029) at 37 °C in 5% CO$_2$ overnight (30).

siRNA Transfection—A combination of four siRNAs (Qiagen, Valencia, CA) were used for silencing LMO4 gene. The siRNA sequences were: Hs_LMO4_8 (catalog no. SI04270966), CGGCACGTCCTGTTACACCAA; Hs_LMO4_9 (catalog no. SI04312973), CCGCCTCTCGCAATATTGCAA; HsLMO4_6 (catalog no. SI03185777), CCCGGGAGATCGGTTTCACTA; Hs_LMO4_7 (catalog no. SI04151231), AGGAAACGTGTTTCAATCAAA. AllStars Negative Control siRNA (Qiagen, catalog no.1027280), CAGGGTATCGACGATTACAAA, was used as a negative control. The transfections were done in Opti-MEM reduced serum medium (Invitrogen, catalog no. 31985) using Oligofectamine (Invitrogen, catalog no. 12252-011) following the manufacturer's protocol. After transfection, the cells or cochlear tissue were incubated for 24 h for silencing the gene and for another 24 h with or without a 10 μM cisplatin treatment. Thus, 48 h after transfection the samples were harvested for Western blot, cell counts, or caspase assay (31).

Caspase Assay—A fluorescein active caspase 3 staining kit (Abcam, Cambridge, MA) was used for detecting activated caspase 3. The cell and cochlea cultures were incubated with FITC-DEVD-FMK reagent (1–3 μl) for 1 h at 37 °C following the manufacturer's protocol. The cells were washed, fixed in cytospin solution (72% isopropyl alcohol, 19% acetone, 7.6% glycerol), and spun onto slides with a Shandon Cytospin II, whereas the cochleae were fixed with 10% buffered formalin and mounted on the slides. The samples were covered with Prolong gold mounting medium containing DAPI (Invitrogen, catalog no. P36935) and were allowed to dry overnight in the dark at room temperature. Images were captured using a Laser Scanning Microscope LSM 510 Meta (Carl Zeiss, Jena, Germany) and analyzed with Zeiss LSM Image Examiner (Version 4.0.0.91).

Cell Counts—Total cells were counted using a Bio-Rad TC10 cell counter. Apoptotic cells were counted using a hemocytometer after trypan blue staining.

RESULTS

Cisplatin Induces Dose-dependent Hearing Loss—Physiological and anatomical measures of hearing were assessed by DPOAE input/output functions and cochleograms, respectively, after treatment with three different doses of cisplatin. DPOAEs were recorded before and 1, 2, and 3 days after treatment with 8, 12, or 16 mg/kg of cisplatin. DPOAE amplitudes with the f2 primary tone of 8 kHz decreased with increasing dose of cisplatin (Fig. 1*A*). A 16-mg/kg dose of cisplatin induced a 10–15-dB decrease in the distortion product amplitude 3 days after treatment. These reductions are consistent with numerous reports of dose- and time-dependent increases in hearing loss after cisplatin treatment (6, 8, 32). Cochleograms obtained 3 days after treatment with 8, 12, or 16 mg/kg of cisplatin showed a dose-dependent increase of OHC loss in the basal region of the cochlea but no IHC loss. The cisplatin-induced OHC loss in the basal turn was mild-to-moderate at the 8 and 12 mg/kg dose, whereas the 16 mg/kg dose induced a massive loss that was almost twice that observed with the 8 or 12 mg/kg dose (Fig. 1*B*). Thus, the functional as well as morphological mea-
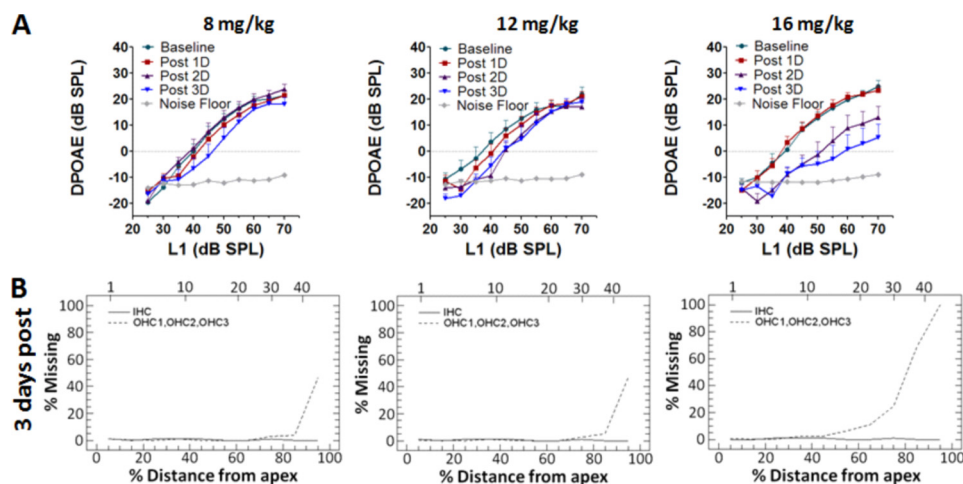
FIGURE 1. **Cisplatin-induced hearing loss.** Cisplatin-induced functional loss assessed by DPOAEs indicated a dose- and time-dependent decrease in DPOAE amplitudes. The traces labeled *base line*, *post 1D*, *2D*, *3D*, *Noise Floor* represent the DPOAEs recorded before, 1 day, 2 days, and 3 days after cisplatin treatment and the noise floor of the DPOAE recordings. The data represent $n = 6$ and are expressed as the means $\pm$ S.E. The cisplatin-induced anatomical loss assessed by the cochleograms indicated a dose-dependent increase in the loss of outer hair cells at the base of the cochlea. Each graph represents the missing hair cells recorded from both the right and left ears of a rat.
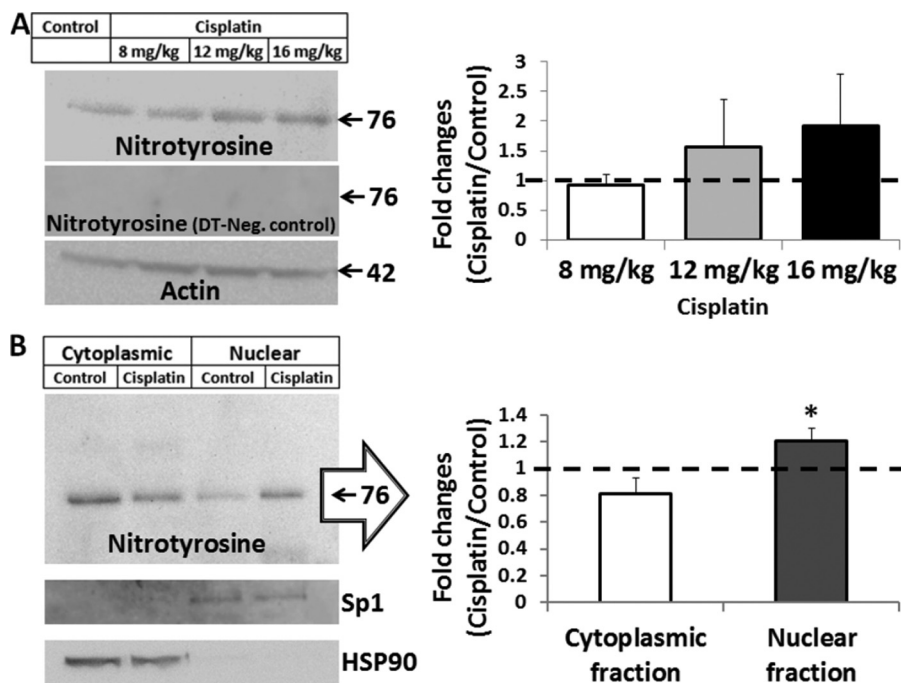

FIGURE 2. **Nitroxidative stress in the cochlea after cisplatin treatment.** *A*, immunoblots indicate that the formation of nitrotyrosine increases in the cochlea with increasing dose of cisplatin 3 days post-treatment ($R^2 = 0.97$, $p < 0.05$). These protein bands were not detected when the membranes were treated with dithionite (*DT*). *B*, differential levels of nitrotyrosine was observed in the cytoplasm and nuclear fractions of the cochlea ($p < 0.05$) when the animals were treated with a 16-mg/kg dose of cisplatin. The immunoblots are representative samples from three biological repeats and were normalized with the expression of actin. Cochlear expression of Sp1 and HSP90 were used as fractionation controls for nuclear and cytoplasmic proteins. The results are expressed as the means $\pm$ S.E., $n = 3$.

sures indicate that cisplatin treatment leads to a dose-dependent loss of OHC that was associated with a decrease in DPOAEs, which depends on the structural integrity of the OHC (33).

Cisplatin Induces Nitration of Proteins in Targets of Cisplatin Ototoxicity—Immunoblots with a monoclonal anti-nitrotyrosine antibody indicated that cisplatin induced a dose-dependent nitration of cochlear proteins ($R^2 = 0.97$, Fig. 2*A*). Although, the most prominent band was detected at 76 kDa 3 days after treatment with cisplatin, the use of monoclonal antibodies might have limited the detection of other potential nitrated proteins. Nevertheless, the dose-dependent increase in nitrotyrosine in the cochlea was strongly correlated with the cisplatin-induced hearing loss ($r = 0.94$), indicative of a link between cochlear protein nitration and cisplatin-mediated ototoxicity. Further analysis of cisplatin-induced formation of nitrotyrosine in subcellular fractions of the cochlea revealed a significant difference ($p < 0.05$) between the cytoplasmic and the nuclear fractions (Fig. 2*B*). The nitrated proteins were increased in the nucleus, whereas they were decreased in the cytoplasm in cisplatin-mediated ototoxicity.
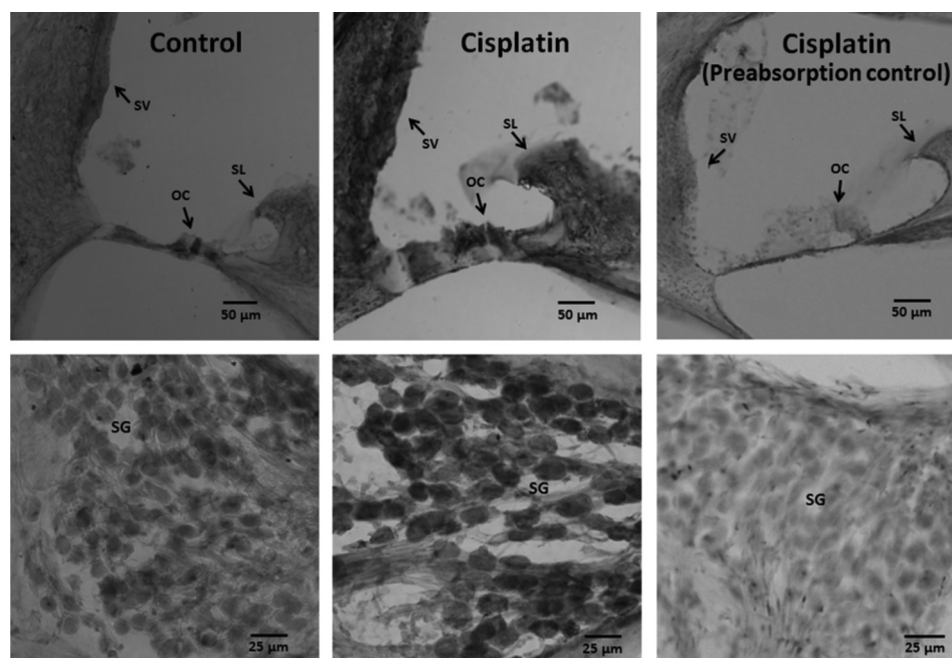
FIGURE 3. **Immunolocalization of nitrated proteins in the cochlea.** Nitrated proteins were localized in the stria vascularis (*SV*), spiral ganglions (*SG*), spiral limbus (*SL*), and organ of corti (*OG*). The staining pattern indicated a darker staining in cisplatin-treated cochlea than the control samples. The specificity of the immunoreaction was indicated by the diminished staining when the antibody was pre-absorbed with nitrotyrosine. The treated animals received a 16-mg/kg dose of cisplatin. The images are representative samples from three biological replicates.
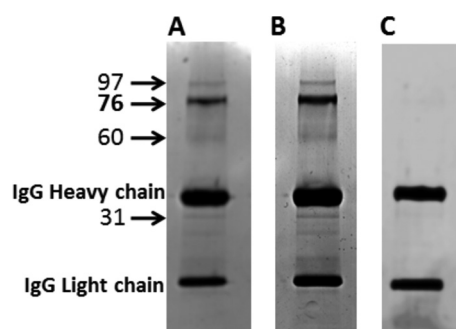

FIGURE 4. **Immunoprecipitation of nitrated cochlear proteins.** Immunoprecipitation of nitrated cochlear proteins using a mouse monoclonal IgG nitrotyrosine antibody bound to magnetic beads revealed that multiple proteins are nitrated in control (*A*) as well as cisplatin (*B*)-treated cochlea. The Coomassie-stained gels indicated an increase in nitrotyrosine in animals that received a 16-mg/kg dose of cisplatin. *C*, the nitrated protein bands were absent in cochlear protein extracts immunoprecipitated with another mouse monoclonal IgG antibody (anti-c-Src). The *numbers* represent the apparent molecular mass in kDa.

Cisplatin-induced increases in nitrated proteins were localized in cryosectioned cochlea with 3′3′-diaminobenzidine tetrahydrochloride staining. An increase in nitrotyrosine was detected in the spiral ganglion, spiral limbus, organ of Corti, and stria vascularis of cisplatin-treated animals (Fig. 3). Immunoprecipitation of cochlear proteins 3 days after treatment with a 16-mg/kg dose of cisplatin with anti-nitrotyrosine revealed four distinct protein bands in each of 6 experiments (Fig. 4). Collectively, these results demonstrate cisplatin-induced nitration of cochlear proteins and highlight the potential significance of protein nitration in cisplatin ototoxicity.

Lmo4 Is Identified as Major Nitrated Cochlear Protein—Identification of the nitrated protein is essential to comprehend the functional implications of nitration in cisplatin ototoxicity. The most prominent protein band detected after immunopre-

cipitation with antinitrotyrosine was digested with trypsin followed by identification of nitrated cochlear protein by MALDI-TOF mass spectrometry. Masses of eight monoisotopic peaks generated using *m/z* software were subjected to peptide mass fingerprinting analysis (Fig. 5). The Mascot search of the NCBI data base for matching peptides resulted in the identification of Lmo4 as the major nitrated cochlear protein with molecular weight search (MOWSE) scores of 89 for Lmo4, isoform CRA_b (*Rattus norvegicus*, gi:149026131) and 73 for LMO4 (*Homo sapiens*, gi:5803072). Protein scores greater than 61 are considered significant. Five masses matched with sequence coverage of 74% for the rat isoform (supplemental Fig. S1).

The nitration site(s) on Lmo4, nitrated by *in vitro* nitration with peroxynitrite, was identified with high confidence by high resolution/accuracy tandem mass spectrometry using the electron-transfer dissociation technique, which is a preferable technique to identify or localize modifications such as tyrosine nitration. Two modified sites were identified on nitrated Lmo4 protein. The nitrated tyrosine residues were localized in the peptides CSCCQAQLGDIGTSCYTKSGMILCR and NDYIRLFGNSGACSACGQSIPASELVMR (supplemental Fig. S2, *A* and *B*). Identification of peroxynitrite-induced nitration of Tyr-65 and Tyr-77 suggests that these two tyrosines of Lmo4 protein are the potential sites of cisplatin-induced nitration of Lmo4.

The identity of Lmo4 and its nitration in cisplatin ototoxicity was confirmed by reciprocal immunoprecipitation and immunoblotting. Nitrated cochlear proteins were precipitated using antibodies against nitrotyrosine and transferred to a PVDF membrane. When this membrane was blotted with antibodies against Lmo4, a 76-kDa protein band was detected suggesting that Lmo4 is one of the nitrated proteins (Fig. 6A). The p60 and p31 did not react with anti-Lmo4 on blots. Under reciprocal conditions, when proteins were precipitated using antibodies
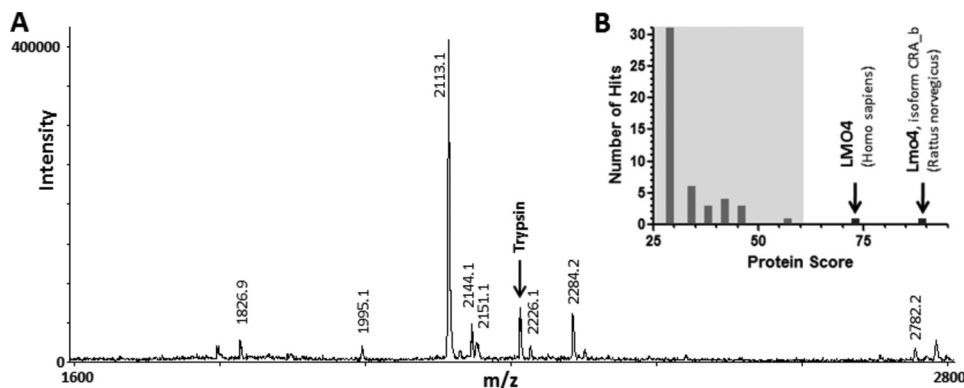
FIGURE 5. **Identification of nitrated cochlear proteins by MALDI TOF mass spectrometry.** *A*, the mass spectrum of nitrated cochlear protein, viewed using *m/z* software, shows the masses of 8 monoisotopic peaks used for peptide mass finger printing. *B*, the Mascot histogram displays the significance levels of the protein scores for two Lmo4 proteins.
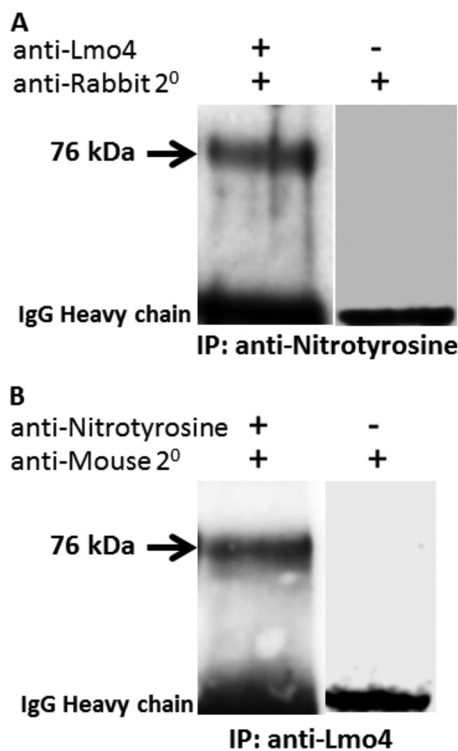

FIGURE 6. **Confirmation of the identity of nitrated Lmo4.** The identity of the nitrated protein was confirmed by reciprocal immunoprecipitation (*IP*) and immunoblotting of cochlear proteins extracted from animals treated with a 16-mg/kg dose of cisplatin. The immunoblot images in *A* and *B* show that the reversal of the nitrotyrosine and Lmo4 antibodies for the two methods resulted in a protein band indicating nitrated Lmo4. When the membrane was stripped and re-probed without the primary antibodies, the nitrated Lmo4 was not detected, although the secondary antibodies detected the IgG bands. The images are representative samples of three biological replicates. The *numbers* represent the apparent molecular mass in kDa.

against Lmo4 and blotted with antibodies against nitrotyrosine, a 76-kDa protein band was also detected suggesting the presence of nitrated Lmo4 (Fig. 6*B*). The 76-kDa band was not detected in the negative controls, where the membranes were probed with just the secondary antibodies. Moreover, the specific detection of protein nitration with this nitrotyrosine antibody was previously indicated by the absence of nitrotyrosine bands in dithionite-treated immunoblots (Fig. 2*A*) and by diminished immunostaining in cryosections probed with pre-

absorbed antibody (Fig. 3). These results confirmed the nitration of Lmo4 in cisplatin mediated ototoxicity.

Nitrotyrosine and Lmo4 Co-localize in Cochlear Targets of Cisplatin Toxicity—Lmo4 and nitrotyrosine co-localized in stria vascularis, spiral ganglion, and organ of Corti in cisplatin-treated rats. In stria vascularis, the intensity of immunofluorescent labeling for nitrotyrosine was greater at the level of marginal cell nuclei compared with that at the level of intermediate and basal cell nuclei. Of the three cell layers, nitrotyrosine labeling was lowest in the basal cell layer. In contrast, Lmo4 was localized to all three layers, but the apparent levels were quite low in the marginal cell layer (Fig. 7*A*). Yellow spots representing the co-registration of nitrotyrosine and Lmo4 were found in some cells in each of these three layers, suggesting the presence of nitrated Lmo4. In the spiral ganglion, Lmo4 was expressed as foci located within the cytoplasm and nucleus and also on the nuclear envelope. Nitrated Lmo4 was almost always observed as single foci attached to or very close to the nuclear envelope (*yellow spots* in the *merged panels* of Fig. 7*B*). In addition, nitrated proteins other than Lmo4 were detected on the plasma membrane of spiral ganglion neurons. Nitrated Lmo4 was higher in the organ of Corti compared with other regions of the cochlea. In supporting cells, nitrated Lmo4 was present either on the nuclear envelope or within the nucleus of Deiters' cells and in the phalangeal processes of pillar cells (Fig. 7*C*). In the region of OHC, nitrated Lmo4 was located within the OHC nucleus, on the nuclear envelope, and in spots 1–2 μm from the nucleus (Fig. 7, *D* and *E*). Nitrated Lmo4 was also detected in the region of IHC and in the inner sulcus. Immunolocalization of nitrated Lmo4 in a single spot on the nuclear envelope was also a common feature in cells of the organ of Corti. In addition to confirming the nitration of Lmo4, the localization of nitrated Lmo4 in the cochlea suggested that Lmo4 nitration has an important role in cisplatin ototoxicity.

Nitroxidative Stress Represses Lmo4 Expression, Which Induces Apoptotic Response—In addition to nitrating Lmo4, cisplatin treatment significantly decreased Lmo4 levels in the cochlea. The 76-kDa Lmo4 immunoreactive protein decreased by 30% 3 days after treatment with 16 mg/kg cisplatin ($p < 0.05$, Fig. 8*A*). In agreement, the intensity of Lmo4 staining of spiral ganglion, spiral ligament, organ of Corti, and stria vascularis was less than that of control animals (Fig. 8*B*). These results
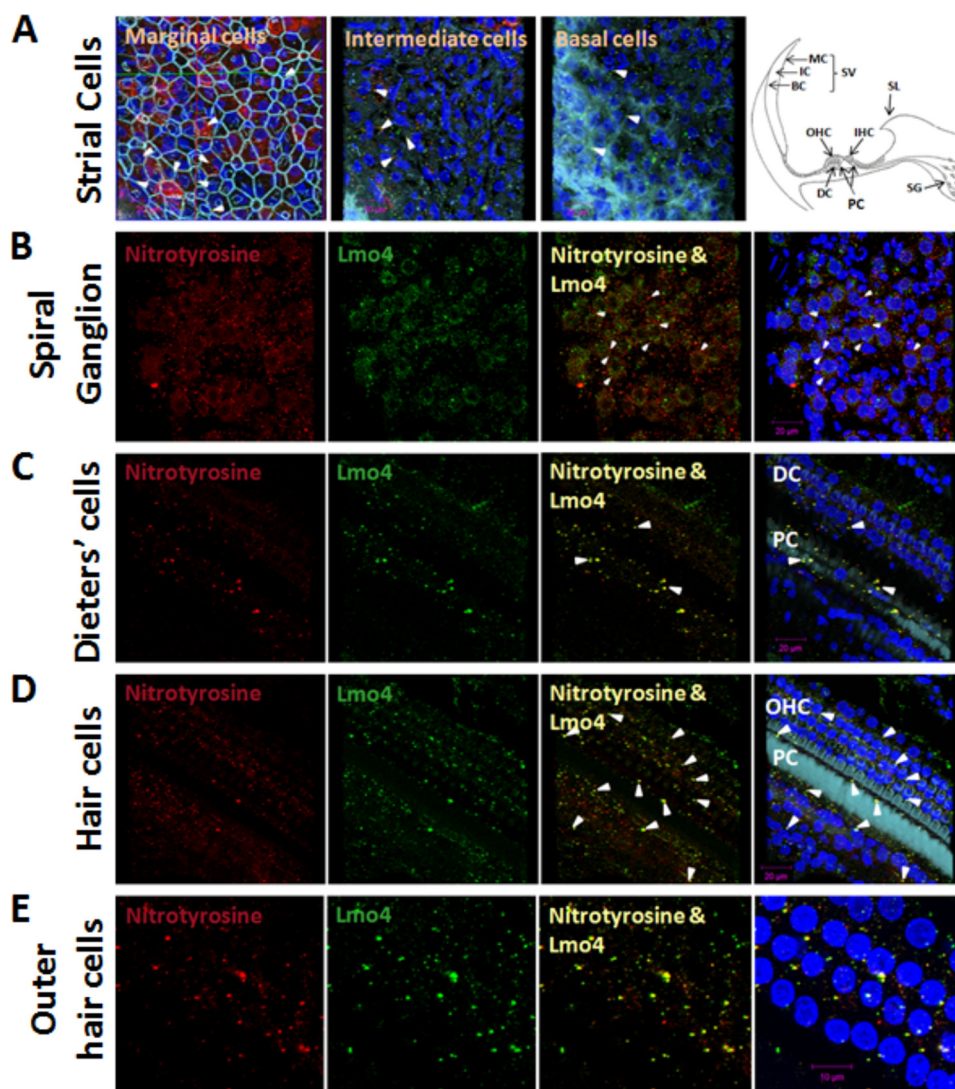
FIGURE 7. **Co-localization of nitrotyrosine and Lmo4 in the cochlea.** Nitrotyrosine and Lmo4 were co-localized in stria vascularis (*SV*; *A*), spiral ganglions (*SG*; *B*), and organ of Corti (*C–E*) in a cisplatin-treated cochlea. *Yellow* indicates immunoreactivity to both nitrotyrosine (*red*) and Lmo4 (*green*), and *light blue* indicates actin staining with phalloidin, whereas the nuclei is stained *blue* with DAPI. The presence of nitrated Lmo4 is indicated by the *white arrows* in some of the cells in all three layers *viz.* marginal cells (*MC*), intermediate cells (*IC*), and basal cells (*BC*) of the stria (*A*) in the spiral ganglions (*B*), in the Dieter's cells (*DC*) and pillar cells (*C*). Co-localization of nitrotyrosine and Lmo4 at the hair cell level demonstrate a much higher immunoreactivity, indicating the presence of nitrated Lmo4 in OHC, IHC, pillar cells, and some cells in the inner sulcus (*D*). The presence of nitrated Lmo4 either in the margins of the nuclei or in the nuclei of almost every OHC is demonstrated in the images taken at a higher magnification (*E*). The spiral limbus (*SL*) is also included in the schematic for orientation of different regions of the cochlea.

suggest that the cisplatin-induced nitration of Lmo4 leads to a decrease in the levels of Lmo4 in the cochlea, although there is a possibility that nitration of Lmo4 may be masking the binding sites of Lmo4 to the antibody. Nevertheless, a significant decrease in the expression of Lmo4 in MDA-MB 231 cells after treatment with 1 mM peroxynitrite ($p < 0.05$, Fig. 9, *A* and *B*) as well as with 10 μM cisplatin ($p < 0.05$, Fig. 10*A*) supports the repression of Lmo4 under nitroxidative conditions.

In addition to repressing Lmo4 expression, peroxynitrite treatment also caused significant cell death ($p < 0.05$, Fig. 9*C*). To further clarify the functional implications of a decrease in Lmo4 levels, the apoptotic responses in cell and cochlear cultures were evaluated after silencing Lmo4 expression. Repression of Lmo4 in MDA-MB 231 cells with siRNA to levels comparable with cisplatin-induced decreases in Lmo4 resulted in a significant decrease in cell counts ($p < 0.01$, Fig. 10*B*) and

increased expression of activated caspase 3, a marker of apoptosis (Fig. 10*C*). Similarly, repression of Lmo4 (36%) in cochlear organotypic cultures with siRNA to levels comparable with cisplatin-induced decreases in Lmo4 (30%), observed *in vivo* studies, resulted in an increase in the expression of activated caspase 3 in the IHC and OHC of the cochlea (Fig. 10, *D* and *E*).

Inhibition of Cisplatin-induced Protein Nitration Attenuates Hearing Loss—Because tyrosine nitration has emerged as a crucial factor in cisplatin ototoxicity, inhibition of cisplatin-induced protein nitration is expected to attenuate cisplatin-induced hearing loss. Trolox (6-hydroxy-2,5,7,8-tetramethylchroman-2-carboxylic acid) is an inhibitor of peroxynitrite (34), and its otoprotective activity has previously been reported (19, 35, 36). Our results provide mechanistic insights into these otoprotective effects by demonstrating that Trolox decreases cisplatin-induced nitration of cochlear proteins ($p <$

0.05, $n = 3$, Fig. 11*A*). In addition to attenuating nitroxidative modification of cochlear proteins, the 100 mg/kg dose of Trolox, administered for 3 days, reversed the cisplatin-induced shift in DPOAE amplitudes ($p < 0.0001$, $n = 6$, Fig. 11*B*). A strong correlation ($r = 0.96$) was observed between nitration of cochlear proteins and shift in distortion product amplitudes. Moreover, Trolox attenuated cisplatin-induced outer hair cell damage in the basal region of the cochlea by nearly 50% (Fig. 11*C*).

DISCUSSION

This study demonstrates the significance of tyrosine nitration in mediating cisplatin ototoxicity by 1) showing a strong correlation between cochlear protein nitration and cisplatin-induced hearing loss and 2) preventing hearing loss by pharmacologic inhibition of protein nitration. These results identify nitroxidative stress as a key mechanism in cisplatin-induced ototoxicity and identify for the first time the nitration of a specific protein, Lmo4, as the major protein that is nitrated during cisplatin treatment. Subsequent immunolocalization studies identified a host of key cochlear structures, in particular the OHC, where considerable protein nitration occurs during cisplatin ototoxicity.

Nitroxidative Stress in Cisplatin-induced Ototoxicity—Nitration of tyrosine is considered as an indicator of oxidative damage to proteins. An increase in cochlear protein nitration has been reported in different animal models after cisplatin treatment (6, 7). This study extends the previous reports on cisplatin-induced nitration by demonstrating a gradual increase in nitration of cochlear proteins with increasing dose of cisplatin. The dose-dependent increase in cochlear protein nitration correlated with a dose-dependent increase in cisplatin-induced ototoxicity, suggesting an important role for protein nitration in ototoxicity. The significant changes observed between cytoplasmic and nuclear fractions further highlights the importance of cochlear protein nitration, as posttranslational modifications such as nitration are capable of causing serious changes in biological function even at minimal levels (37). In addition, the localization of nitrated proteins in known targets of cisplatin toxicity, particularly OHC, emphasized the importance of nitration in mediating ototoxicity after cisplatin treatment.

Nitration of Lmo4 in Cisplatin Toxicity—The number of proteins known to be modified by nitration is relatively small (38). Although previous reports have indicated nitration of cochlear proteins in cisplatin ototoxicity, this is the first study to actually confirm the identity of a nitrated cochlear protein. Multiple nitrated proteins were detected in cisplatin-treated cochlea. The most prominent nitrated protein band was identified as Lmo4 by in-gel tryptic digestion followed by MALDI-TOF mass spectrometry and mass fingerprinting. Analysis of nitrated Lmo4 by tandem mass spectrometry identified Tyr-65 and Tyr-77 as sites of modification. The nitration of Lmo4 in cisplatin-mediated ototoxicity was confirmed by reciprocal immunoprecipitation and immunoblotting with antibodies against nitrotyrosine and Lmo4.

Lmo4 is a transcriptional regulator and is considered to be an oncogene. Being a molecular adaptor for protein-protein interactions, it is a scaffold for protein complexes and binds with
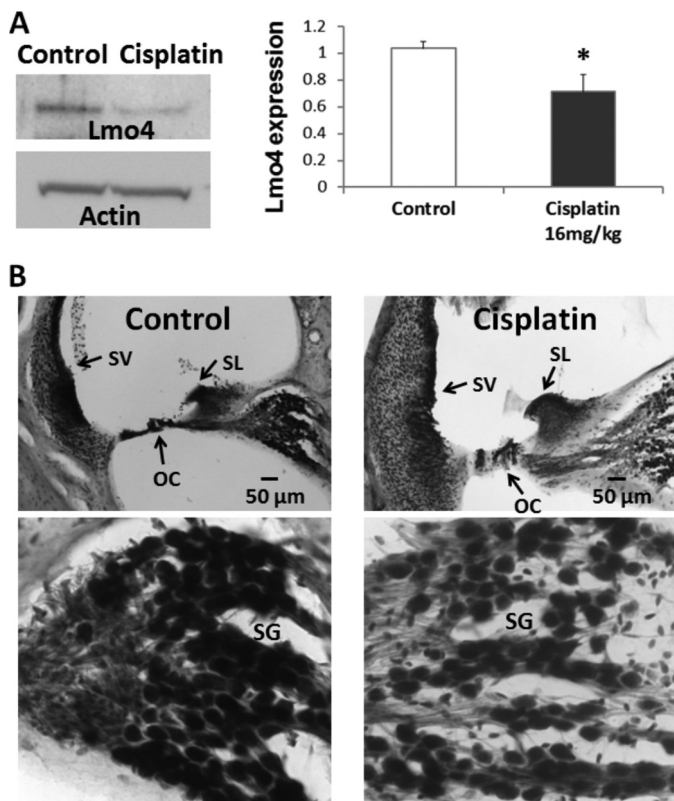

FIGURE 8. **Expression of Lmo4 in the cochlea.** *A*, cisplatin-induced decrease in the expression levels of Lmo4 was demonstrated by immunoblots with a polyclonal antibody against Lmo4 ($p < 0.05$). The immunoblot images are representative samples of six biological repeats. *B*, localization of Lmo4 in the cochlea revealed Lmo4 immunoreactivity in stria vascularis (*SV*), spiral limbus (*SL*), spiral ganglions (*SG*), and organ of Corti (*OG*). Consistent with the immunoblots, the control samples showed a darker staining pattern than the cisplatin-treated samples. The treated animals received a 16-mg/kg dose of cisplatin. The images are representative samples of three biological replicates.
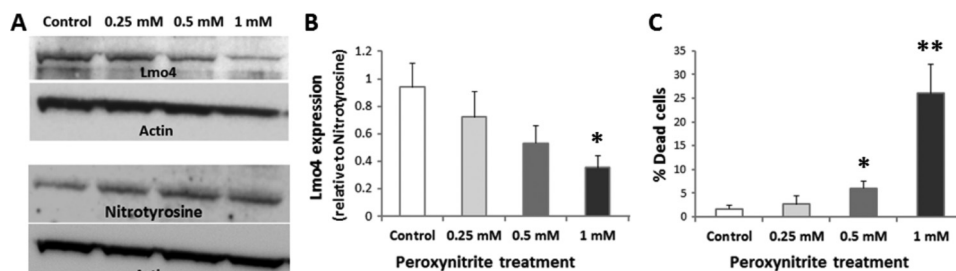

FIGURE 9. **Nitroxidative stress represses Lmo4 expression.** *A*, treatment with peroxynitrite (0.25, 0.5, and 1 mM) showed a tendency to increase the levels of nitrotyrosine despite the decreases observed in corresponding Lmo4 substrates in MDA-MB-231 cells. *B*, a significant decrease in the expression of Lmo4 was detected with 1 mM peroxynitrite treatment ($p < 0.05$). *C*, the number of dead cells, detected using trypan blue stain, also increased significantly with 0.5 mM ($p < 0.05$) and 1 mM ($p < 0.01$) peroxynitrite treatment.
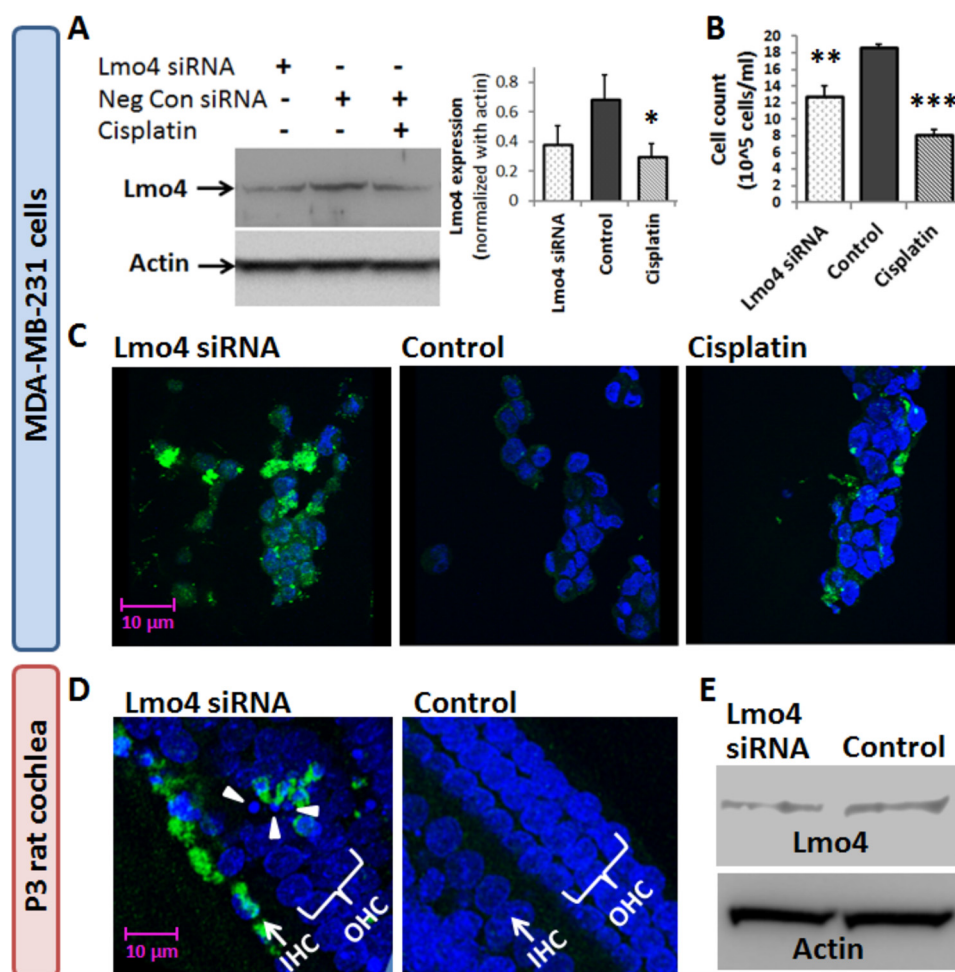
FIGURE 10. **Repression of Lmo4 induces apoptosis.** *A*, immunoblots indicate that Lmo4 siRNA transfection repressed the expression of Lmo4 in MDA-MB-231 cells to levels that were comparable with cisplatin-induced decrease in the expression of Lmo4. *B*, significant reduction in cell counts was observed after siRNA as well as cisplatin treatment. *C*, immunolabeling of activated caspase 3 (*green*) indicated that an apoptotic response accompanied the decrease in Lmo4 levels in siRNA- or cisplatin-treated cells. DAPI (*blue*) was used to stain the nuclei. *D*, consistent with the cell line studies, a similar apoptotic response was observed in the hair cells of the P3 rat cochlea, indicated by an increase in activated caspase 3 labeling and the presence of condensed nuclei (*arrows*) after repression of Lmo4 with siRNA. *E*, immunoblots showed that siRNA treatment decreased the cochlear expression of Lmo4 by about 30%, which was comparable with the cisplatin-induced decrease in Lmo4 observed in the *in vivo* studies (Fig. 8). Cochleae from three P3 rats were pooled together for the immunoblots, whereas all other experiments were repeated in three biological replicates. The results are expressed as the means ± S.E., $n = 3$.
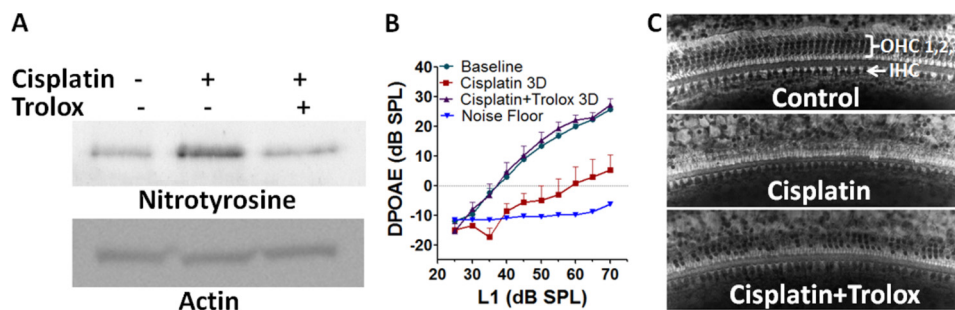
FIGURE 11. **Attenuation of cochlear protein nitration prevents cisplatin-induced hearing loss.** *A*, Trolox treatment decreased the cisplatin-induced nitration of cochlear proteins. The immunoblots are representative samples from three biological replicates. The cochlear nitrotyrosine was normalized with expression of actin. *B*, prevention of cisplatin-induced hearing loss by Trolox is shown. Cisplatin treatment reduced DPOAE amplitudes (means ± S.E., $n = 6$); DPOAE amplitude was essentially normal after combined treatment with Trolox plus cisplatin. *C*, shown are representative photomicrographs of the basal turn of the organ of Corti. Most of the OHC are missing in cisplatin-treated animals compared with control. Almost 50% more outer hair cells were in cisplatin plus Trolox-treated animals than cisplatin alone. The cochlear images are representative samples from two animals for each group.

several transcription factors and co-regulators (39, 40). It controls gene expression by modulating the formation of transcriptional complexes and represses or promotes transcription (31, 40–42). Studies of Lmo4 expression in the inner ear are relatively new. In mice with targeted gene disruption, Lmo4 was

associated with malformation of inner ear development, particularly vestibular morphogenesis (43). To the best of our knowledge, there are no reports of its expression pattern in the adult cochlea, its association with any auditory pathology, or its nitration by cochlear stressors. Nevertheless, cisplatin induced an

increase in Lmo4 nitration, decreased total Lmo4 immunoblot levels, and decreased Lmo4 staining patterns in the cochlea. Moreover, repression of Lmo4 under nitroxidative conditions also induced an apoptotic response. These data and previous reports indicating degradation of nitrated proteins by the 20 S proteasome (16, 17) suggest that increased nitration and decreased levels of Lmo4 are both likely to alter functional mechanisms that regulate Lmo4 transcriptional activity, *e.g.* tyrosine phosphorylation, protein-protein, and protein-DNA interaction.

Functional Role of Lmo4 in Mediating Cisplatin Toxicity—Silencing of Lmo4 expression to levels comparable with cisplatin-induced decreases in Lmo4 leads to an increased expression of activated caspase 3 in breast cancer cells and hair cells of the cochlea. These results suggest that the cisplatin-induced decrease in Lmo4 is an important factor in mediating the apoptotic responses of the cochlea. Although the association of nitration of Lmo4 and cell death supports a role for this transcriptional regulator in decisions of cell survival and cell death, the experiments using siRNA to silence Lmo4 provide stronger support for this hypothesis. Moreover, the characteristics of Lmo4 and its interacting proteins and target genes also imply a role for Lmo4 nitration in cisplatin ototoxicity. Estrogen receptor, an Lmo4 interacting protein, is abundantly expressed in the cochlea (44) and is considered to have an important functional role in the auditory system (45). Lmo4 binds to estrogen receptor α and represses its transactivation activities (31). Cisplatin-induced modulation of Lmo4 can facilitate the inhibition of Stat3 activity by a direct physical interaction of estrogen receptor α with Stat3 (46). Moreover, silencing of Lmo4 expression decreases Stat3 activity (47) as Lmo4 mediates ATP signaling that leads to phosphorylation of Stat3 (48). Because inhibition of Stat3 activity has been implicated in drug-mediated apoptosis (49, 50), decreases in cochlear ATP (14) and Lmo4 levels after cisplatin treatment point to the significance of Lmo4 in mediating an apoptotic response. Therefore, it can be hypothesized that cisplatin-induced nitration of Lmo4 leads to a decrease in the expression of Lmo4 and subsequently reduces Stat3 activity, thereby contributing to cisplatin-mediated apoptosis in the hair cells of cochlea.

Alternatively, Lmo4 could play a role in promoting a survival response in other cell types of the cochlea through multiple mechanisms. First, cisplatin-induced nitration of Lmo4 and a subsequent decrease in the expression of Lmo4 could facilitate DNA repair through its interaction with BRCA1 and RBBP8. BRCA1, a tumor suppressor protein, is repressed by its direct interaction with Lmo4 and forms a multiprotein complex along with RBBP8 and LDB1 (40). RBBP8 and BRCA1 are both required for repair of double-strand breaks (51). Second, Lmo4 has been reported to bind with HEN1 and modulate its transcriptional activity, resulting in the inhibition of neurite extension (39). Thus, decreased Lmo4 levels and activity can promote neuron function. Third, Lmo4 can also inhibit neurite outgrowth and prevent regeneration of neurons after injury through its interaction with neogenin, a receptor for repulsive guidance molecule A (52). Despite these multiple possibilities, the specific mechanism by which Lmo4 mediates its activity will depend on the availability of binding partners and whether the nitration of Lmo4 influences its binding with specific partners.

OHC are the primary targets of cisplatin ototoxicity. Immunoreactivity indicating the presence of nitrated Lmo4 was more pronounced in the hair cell nuclei when compared with other regions of the cochlea. Nuclear association of nitrated Lmo4 in every single OHC highlights the functional significance of this posttranslational modification in cisplatin ototoxicity. Because Lmo4 is also expressed in other cell types, it will be interesting to establish the cellular distribution of Lmo4 nuclear binding partners. Lmo4 may have different roles in different cell types depending on the expression level of specific interacting proteins. Our working hypothesis favors a toxic role in hair cells involving mediation of cell death rather than a protective role promoting DNA repair.

Inhibition of Cochlear Protein Nitration and Attenuation of Cisplatin-induced Hearing Loss—Prevention of cisplatin-induced hearing loss through inhibition of protein nitration demonstrates the critical role cochlear protein nitration plays in cisplatin ototoxicity. As noted earlier, Trolox inhibits peroxynitrite-mediated oxidative stress and apoptosis in thymocytes (34) and alleviates cisplatin-induced renal (19) and neuronal apoptosis (53). Moreover, treatment with Trolox has been shown to protect against cisplatin ototoxicity (35). Consistent with earlier reports, our results show a strong correlation between Trolox treatment and the attenuation of cisplatin-induced cochlear protein nitration as well as the attenuation of the cisplatin-induced DPOAE loss. In addition, a marked reduction in cisplatin-induced hair cell loss was observed after Trolox treatment. These results highlight the importance of cochlear protein nitration in cisplatin ototoxicity.

The overall findings of this study indicate that nitroxidative modification of cochlear proteins plays a crucial role in cisplatin ototoxicity, and Lmo4 appears to be a key player in mediating the cochlear pathology. Characterization of nitroxidative stress and particularly demonstration of Lmo4 nitration is of great significance as it points to many new target genes related to stress responses. Further analysis of Lmo4 interactomes shall reveal the exact molecular mechanism by which nitration of Lmo4 leads to hair cell loss in cisplatin ototoxicity.

REFERENCES

1. Dehne, N., Lautermann, J., Petrat, F., Rauen, U., and de Groot, H. (2001) Cisplatin ototoxicity. Involvement of iron and enhanced formation of superoxide anion radicals. *Toxicol. Appl. Pharmacol.* **174,** 27–34
2. Berndtsson, M., Hägg, M., Panaretakis, T., Havelka, A. M., Shoshan, M. C., and Linder, S. (2007) Acute apoptosis by cisplatin requires induction of reactive oxygen species but is not associated with damage to nuclear DNA. *Int. J. Cancer* **120,** 175–180
3. Bánfi, B., Malgrange, B., Knisz, J., Steger, K., Dubois-Dauphin, M., and Krause, K. H. (2004) NOX3, a superoxide-generating NADPH oxidase of the inner ear. *J. Biol. Chem.* **279,** 46065–46072
4. Radi, R., Peluffo, G., Alvarez, M. N., Naviliat, M., and Cayota, A. (2001) Unraveling peroxynitrite formation in biological systems. *Free Radic. Biol. Med.* **30,** 463–488
5. van der Vliet, A., Eiserich, J. P., Halliwell, B., and Cross, C. E. (1997) For-

mation of reactive nitrogen species during peroxidase-catalyzed oxidation of nitrite. A potential additional mechanism of nitric oxide-dependent toxicity. *J. Biol. Chem.* **272,** 7617–7625

6. Jamesdaniel, S., Ding, D., Kermany, M. H., Davidson, B. A., Knight, P. R., 3rd, Salvi, R., and Coling, D. E. (2008) Proteomic analysis of the balance between survival and cell death responses in cisplatin-mediated ototoxicity. *J. Proteome Res.* **7,** 3516–3524

7. Lee, J. E., Nakagawa, T., Kim, T. S., Endo, T., Shiga, A., Iguchi, F., Lee, S. H., and Ito, J. (2004) Role of reactive radicals in degeneration of the auditory system of mice after cisplatin treatment. *Acta Otolaryngol.* **124,** 1131–1135

8. Rybak, L. P., Whitworth, C. A., Mukherjea, D., and Ramkumar, V. (2007) Mechanisms of cisplatin-induced ototoxicity and prevention. *Hear. Res.* **226,** 157–167

9. van Ruijven, M. W., de Groot, J. C., Hendriksen, F., and Smoorenburg, G. F. (2005) Immunohistochemical detection of platinated DNA in the cochlea of cisplatin-treated guinea pigs. *Hear. Res.* **203,** 112–121

10. Meech, R. P., Campbell, K. C., Hughes, L. P., and Rybak, L. P. (1998) A semiquantitative analysis of the effects of cisplatin on the rat stria vascularis. *Hear. Res.* **124,** 44–59

11. Ravi, R., Somani, S. M., and Rybak, L. P. (1995) Mechanism of cisplatin ototoxicity. Antioxidant system. *Pharmacol. Toxicol.* **76,** 386–394

12. van Ruijven, M. W., de Groot, J. C., Klis, S. F., and Smoorenburg, G. F. (2005) The cochlear targets of cisplatin. An electrophysiological and morphological time-sequence study. *Hear. Res.* **205,** 241–248

13. Anniko, M., and Sobin, A. (1986) Cisplatin. Evaluation of its ototoxic potential. *Am. J. Otolaryngol.* **7,** 276–293

14. García-Berrocal, J. R., Nevado, J., Ramírez-Camacho, R., Sanz, R., González-García, J. A., Sánchez-Rodríguez, C., Cantos, B., España, P., Verdaguer, J. M., and Trinidad Cabezas, A. (2007) The anticancer drug cisplatin induces an intrinsic apoptotic pathway inside the inner ear. *Br. J. Pharmacol.* **152,** 1012–1020

15. Kong, S. K., Yim, M. B., Stadtman, E. R., and Chock, P. B. (1996) Peroxynitrite disables the tyrosine phosphorylation regulatory mechanism. Lymphocyte-specific tyrosine kinase fails to phosphorylate nitrated cdc2(6–20)NH2 peptide. *Proc. Natl. Acad. Sci. U.S.A.* **93,** 3377–3382

16. Gow, A. J., Duran, D., Malcolm, S., and Ischiropoulos, H. (1996) Effects of peroxynitrite-induced protein modifications on tyrosine phosphorylation and degradation. *FEBS Lett.* **385,** 63–66

17. Kim, J. Y., Song, E. H., Lee, H. J., Oh, Y. K., Park, Y. S., Park, J. W., Kim, B. J., Kim, D. J., Lee, I., Song, J., and Kim, W. H. (2010) Chronic ethanol consumption-induced pancreatic β-cell dysfunction and apoptosis through glucokinase nitration and its down-regulation. *J. Biol. Chem.* **285,** 37251–37262

18. Kelly, T. C., Whitworth, C. A., Husain, K., and Rybak, L. P. (2003) Aminoguanidine reduces cisplatin ototoxicity. *Hear. Res.* **186,** 10–16

19. Maruyama, J., Miller, J. M., and Ulfendahl, M. (2008) Glial cell line-derived neurotrophic factor and antioxidants preserve the electrical responsiveness of the spiral ganglion neurons after experimentally induced deafness. *Neurobiol. Dis.* **29,** 14–21

20. Ding, D., McFadden, S., and Salvi, R. J. (2001) Cochlear hair cell densities and inner ear staining techniques. In *The Auditory Psychobiology of the Mouse* (Willott, J. F. ed.) pp 189–204, CRC Press, Boca Raton, FL

21. Bradford, M. M. (1976) A rapid and sensitive method for the quantitation of microgram quantities of protein utilizing the principle of protein-dye binding. *Anal. Biochem.* **72,** 248–254

22. Xu, S., Ying, J., Jiang, B., Guo, W., Adachi, T., Sharov, V., Lazar, H., Menzoian, J., Knyushko, T. V., Bigelow, D., Schöneich, C., and Cohen, R. A. (2006) Detection of sequence-specific tyrosine nitration of manganese SOD and SERCA in cardiovascular disease and aging. *Am. J. Physiol. Heart Circ. Physiol.* **290,** H2220–H2227

23. Coling, D., and Kachar, B. (2001) Theory and application of fluorescence microscopy. *Curr. Protoc. Neurosci.* Chapter 2, Unit 2.1

24. Coling, D. E., Ding, D., Young, R., Lis, M., Stofko, E., Blumenthal, K. M., and Salvi, R. J. (2007) Proteomic analysis of cisplatin-induced cochlear damage. Methods and early changes in protein expression. *Hear. Res.* **226,** 140–156

25. Wang, Y., Luo, Y., Zhong, R., Gao, D., and Cui, S. (2008) Identification of

26. Duan, X., Young, R., Straubinger, R. M., Page, B., Cao, J., Wang, H., Yu, H., Canty, J. M., and Qu, J. (2009) A straightforward and highly efficient precipitation/on-pellet digestion procedure coupled with a long gradient nano-LC separation and Orbitrap mass spectrometry for label-free expression profiling of the swine heart mitochondrial proteome. *J. Proteome Res.* **8,** 2838–2850

27. Tu, C., Li, J., Young, R., Page, B. J., Engler, F., Halfon, M. S., Canty, J. M., Jr., and Qu, J. (2011) Combinatorial peptide ligand library treatment followed by a dual-enzyme, dual-activation approach on a nanoflow liquid chromatography/orbitrap/electron transfer dissociation system for comprehensive analysis of swine plasma proteome. *Anal. Chem.* **83,** 4802–4813

28. Wang, H., Straubinger, R. M., Aletta, J. M., Cao, J., Duan, X., Yu, H., and Qu, J. (2009) Accurate localization and relative quantification of arginine methylation using nanoflow liquid chromatography coupled to electron transfer dissociation and orbitrap mass spectrometry. *J. Am. Soc. Mass. Spectrom.* **20,** 507–519

29. Cassina, P., Peluffo, H., Pehar, M., Martinez-Palma, L., Ressia, A., Beckman, J. S., Estévez, A. G., and Barbeito, L. (2002) Peroxynitrite triggers a phenotypic transformation in spinal cord astrocytes that induces motor neuron apoptosis. *J. Neurosci. Res.* **67,** 21–29

30. Ding, D., He, J., Allman, B. L., Yu, D., Jiang, H., Seigel, G. M., and Salvi, R. J. (2011) Cisplatin ototoxicity in rat cochlear organotypic cultures. *Hear. Res.* **282,** 196–203

31. Singh, R. R., Barnes, C. J., Talukder, A. H., Fuqua, S. A., and Kumar, R. (2005) Negative regulation of estrogen receptor α transactivation functions by LIM domain only 4 protein. *Cancer Res.* **65,** 10594–10601

32. Campbell, K. C., Meech, R. P., Klemens, J. J., Gerberi, M. T., Dyrstad, S. S., Larsen, D. L., Mitchell, D. L., El-Azizi, M., Verhulst, S. J., and Hughes, L. F. (2007) Prevention of noise- and drug-induced hearing loss with D-methionine. *Hear. Res.* **226,** 92–103

33. Hofstetter, P., Ding, D., Powers, N., and Salvi, R. J. (1997) Quantitative relationship of carboplatin dose to magnitude of inner and outer hair cell loss and the reduction in distortion product otoacoustic emission amplitude in chinchillas. *Hear. Res.* **112,** 199–215

34. Hogg, N., Joseph, J., and Kalyanaraman, B. (1994) The oxidation of α-tocopherol and trolox by peroxynitrite. *Arch. Biochem. Biophys.* **314,** 153–158

35. Teranishi, M. A., and Nakashima, T. (2003) Effects of trolox, locally applied on round windows, on cisplatin-induced ototoxicity in guinea pigs. *Int. J. Pediatr. Otorhinolaryngol.* **67,** 133–139

36. Yamashita, D., Jiang, H. Y., Le Prell, C. G., Schacht, J., and Miller, J. M. (2005) Post-exposure treatment attenuates noise-induced hearing loss. *Neuroscience* **134,** 633–642

37. Ischiropoulos, H. (2003) Biological selectivity and functional aspects of protein tyrosine nitration. *Biochem. Biophys. Res. Commun.* **305,** 776–783

38. Souza, J. M., Peluffo, G., and Radi, R. (2008) Protein tyrosine nitration. Functional alteration or just a biomarker? *Free. Radic. Biol. Med.* **45,** 357–366

39. Manetopoulos, C., Hansson, A., Karlsson, J., Jönsson, J. I., and Axelson, H. (2003) The LIM-only protein LMO4 modulates the transcriptional activity of HEN1. *Biochem. Biophys. Res. Commun.* **307,** 891–899

40. Sum, E. Y., Peng, B., Yu, X., Chen, J., Byrne, J., Lindeman, G. J., and Visvader, J. E. (2002) The LIM domain protein LMO4 interacts with the cofactor CtIP and the tumor suppressor BRCA1 and inhibits BRCA1 activity. *J. Biol. Chem.* **277,** 7849–7856

41. Setogawa, T., Shinozaki-Yabana, S., Masuda, T., Matsuura, K., and Akiyama, T. (2006) The tumor suppressor LKB1 induces p21 expression in collaboration with LMO4, GATA-6, and Ldb1. *Biochem. Biophys. Res. Commun.* **343,** 1186–1190

42. Wang, N., Lin, K. K., Lu, Z., Lam, K. S., Newton, R., Xu, X., Yu, Z., Gill, G. N., and Andersen, B. (2007) The LIM-only factor LMO4 regulates expression of the BMP7 gene through an HDAC2-dependent mechanism and controls cell proliferation and apoptosis of mammary epithelial cells. *Oncogene* **26,** 6431–6441

43. Deng, M., Pan, L., Xie, X., and Gan, L. (2010) Requirement for Lmo4 in the vestibular morphogenesis of mouse inner ear. *Dev. Biol.* **338,** 38–49

44. Jamesdaniel, S., Ding, D., Kermany, M. H., Jiang, H., Salvi, R., and Coling,

25. Wang, Y., Luo, Y., Zhong, R., Gao, D., and Cui, S. (2008) Identification of

ASBMB

D. (2009) Analysis of cochlear protein profiles of Wistar, Sprague-Dawley, and Fischer 344 rats with normal hearing function. *J. Proteome Res.* **8,** 3520–3528

45. Charitidi, K., and Canlon, B. (2010) Estrogen receptors in the central auditory system of male and female mice. *Neuroscience* **165,** 923–933

46. Yamamoto, T., Matsuda, T., Junicho, A., Kishi, H., Saatcioglu, F., and Muraguchi, A. (2000) Cross-talk between signal transducer and activator of transcription 3 and estrogen receptor signaling. *FEBS Lett.* **486,** 143–148

47. Novotny-Diermayr, V., Lin, B., Gu, L., and Cao, X. (2005) Modulation of the interleukin-6 receptor subunit glycoprotein 130 complex and its signaling by LMO4 interaction. *J. Biol. Chem.* **280,** 12747–12757

48. Chen, H. H., Schock, S. C., Xu, J., Safarpour, F., Thompson, C. S., and Stewart, A. F. (2007) Extracellular ATP-dependent up-regulation of the transcription cofactor LMO4 promotes neuron survival from hypoxia. *Exp. Cell Res.* **313,** 3106–3116

49. Lee, J., Hahm, E. R., and Singh, S. V. (2010) Withaferin A inhibits activation of signal transducer and activator of transcription 3 in human breast cancer cells. *Carcinogenesis* **31,** 1991–1998

50. Zhao, W., Zhang, T., Qu, B., Wu, X., Zhu, X., Meng, F., Gu, Y., Shu, Y., Shen, Y., Sun, Y., and Xu, Q. (2011) Sorafenib induces apoptosis in HL60 cells by inhibiting Src kinase-mediated STAT3 phosphorylation. *Anticancer Drugs* **22,** 79–88

51. Yun, M. H., and Hiom, K. (2009) CtIP-BRCA1 modulates the choice of DNA double-strand-break repair pathway throughout the cell cycle. *Nature* **459,** 460–463

52. Schaffar, G., Taniguchi, J., Brodbeck, T., Meyer, A. H., Schmidt, M., Yamashita, T., and Mueller, B. K. (2008) LIM-only protein 4 interacts directly with the repulsive guidance molecule A receptor neogenin. *J. Neurochem.* **107,** 418–431

53. Xiao, T., Choudhary, S., Zhang, W., Ansari, N. H., and Salahudeen, A. (2003) Possible involvement of oxidative stress in cisplatin-induced apoptosis in LLC-PK1 cells. *J. Toxicol. Environ. Health A.* **66,** 469–479